Chiral Tunneling in a Twisted Graphene Bilayer

Wen-Yu He, Zhao-Dong Chu, and Lin He*

Department of Physics, Beijing Normal University, Beijing, 100875, People's Republic of China

(Received 31 January 2013; published 6 August 2013)

The perfect transmission in a graphene monolayer and the perfect reflection in a Bernal graphene bilayer for electrons incident in the normal direction of a potential barrier are viewed as two incarnations of the Klein paradox. Here we show a new and unique incarnation of the Klein paradox. Owing to the different chiralities of the quasiparticles involved, the chiral fermions in a twisted graphene bilayer show an adjustable probability of chiral tunneling for normal incidence: they can be changed from perfect tunneling to partial or perfect reflection, or vice versa, by controlling either the height of the barrier or the incident energy. As well as addressing basic physics about how the chiral fermions with different chiralities tunnel through a barrier, our results provide a facile route to tune the electronic properties of the twisted graphene bilayer.

DOI: 10.1103/PhysRevLett.111.066803 PACS numbers: 73.22.Pr, 73.40.Gk, 73.61.Wp

Because of graphene's two-dimensional honeycomb lattice, quasiparticles in graphene mimic Dirac fermions in quantum electrodynamics (QED) [1–8]. Therefore, this condensed-matter system is expected to help demonstrate many oddball effects predicted by QED. One example is the Klein paradox [9–11]. The chirality of the charge carriers in a graphene monolayer ensures perfect quantum tunneling for electrons incident in the normal direction of a potential barrier [9,10]. This is viewed as a direct experimental test of the Klein's gedanken experiment [11]. In light of possible applications, the chirality suppresses backscattering of quasiparticles and protects high charge carrier mobility of graphene despite unavoidable inhomogeneities [3,12,13]. The emergence of superlattice Dirac points in a graphene superlattice, as reported very recently [14–16], is also directly related to the chiral nature of the Dirac fermions [17–20]. Owing to the different chiralities of the quasiparticles involved, the quantum tunneling in the Bernal graphene bilayer leads to the opposite effect: massive chiral fermions are always perfectly reflected for a sufficiently wide barrier for normal incidence [9]. This result implies that it may be possible to find different chiral fermions in a graphene system to show "designable" tunneling properties. In this Letter, we will demonstrate subsequently that a twisted graphene bilayer is a good candidate to achieve this goal. The chiral fermions in twisted graphene bilayers show the adjustable probability of chiral tunneling for a normal incidence. The transmission probability can be changed between 1 and 0 by controlling either the height of the barrier or the incident energy. This unique tunneling behavior is of potential application in designing future electronic devices.

Figure 1(a) shows the general scheme where a chiral electron starts penetrating through a potential barrier $U(x)$, which has a rectangular shape with width D and height $E + \Delta U$ (here E is the incident energy of the electron, ΔU is the energy difference between the potential barrier and the incident energy). The potential barrier is infinite along the y axis. The rectangular shape assumption of the barrier means that the characteristic width of the edge smearing is much smaller than the electron wavelength, but much larger than the lattice constant. Such an assumption disallows scattering to mix the two valleys in graphene and,

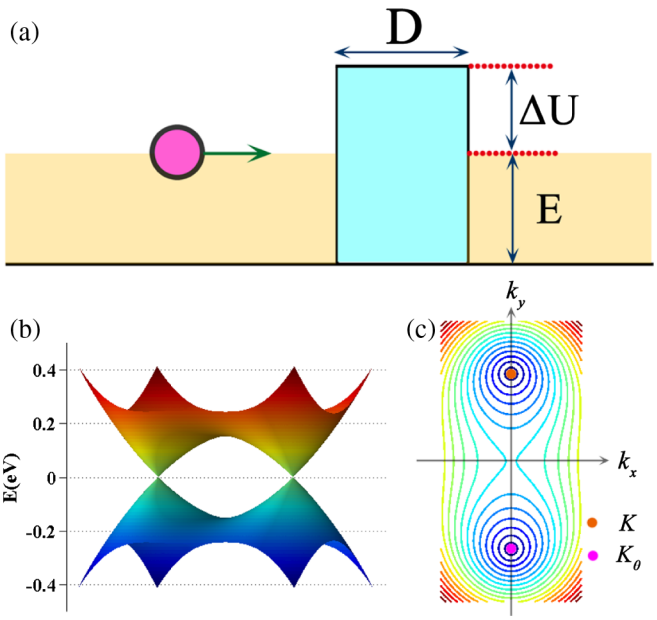

FIG. 1 (color online). Tunneling through a barrier in a twisted graphene bilayer. (a) Schematic diagram of an electron coming to a potential-energy barrier of height $E + \Delta U$ and width D. E is the Fermi energy of the twisted graphene bilayer and the one-dimensional barrier is infinite along the y direction. (b) Electronic spectrum of the quasiparticles in a twisted graphene bilayer with a finite interlayer coupling in the proximity of one of the two valleys. Two saddle points form between the two Dirac cones, K and K_θ. (c) Density plot of the energy dispersion of the twisted graphene bilayer around K and K_θ. k_x is the direction perpendicular to the barrier.

consequently, we only need to consider scattering electrons from one valley [9]. This tunneling problem was first considered in Ref. [9] for chiral electrons in a graphene monolayer and a Bernal graphene bilayer. This system can be divided into three distinct regions: the left of the barrier ($x < 0$), inside the barrier ($0 < x < D$), and the right of the barrier ($x > D$). If we know the wave functions in the three regions, then it is straightforward to solve this tunneling problem. For a twisted graphene bilayer, the Dirac points of the two layers no longer coincide and the zero energy states occur at $\vec{k} = -(\Delta K_x/2, \Delta K_y/2)$ and $\vec{k} = (\Delta K_x/2, \Delta K_y/2)$ in layer 1 and 2, respectively. Here $(\Delta K_x, \Delta K_y)$ is the relative shift between the corresponding Dirac points of the twisted graphene bilayer. Its modulus is $2|\vec{K}|\sin(\theta/2)$ with $|\vec{K}| = 4\pi/3a$ and a ~0.246 nm the lattice constant of the hexagonal lattice. The displaced Dirac cones of the twisted bilayer cross and two intersections of the saddle points along the two cones appear in the presence of interlayer coupling $t_\perp$ [21,22], as shown in Figs. 1(b) and 1(c). The saddle points result in two low-energy van Hove singularities (VHSs) at $\pm E_V = \pm 1/2(\hbar\nu_F|\Delta K| - 2t_\perp)$ in the density of states (here $\nu_F \sim 1.0 \times 10^6$ m/s is the Fermi velocity). The band structure of the twisted graphene bilayer was subsequently confirmed experimentally by Raman spectroscopy, scanning tunneling spectroscopy, and angle-resolved photoemission spectroscopy [15,23–28]. Theoretically, it was predicted that electron-electron interaction in the Bernal graphene bilayer will split the quadratic band touch point into two Dirac points and result in similar energy dispersion as that of a twisted graphene bilayer (it was denoted as a nematic broken symmetry state in the Bernal graphene bilayer) [29–31].

When we consider only low-energy excitations, the effective Hamiltonian of the twisted graphene bilayer can be described by [21,22,32,33]

$$H^{\text{eff}} = -\frac{2\nu_F^2}{15\tilde{t}_\perp}\begin{pmatrix} 0 & (k^*)^2 - \left(\frac{1}{2}\Delta K^*\right)^2 \\ k^2 - \left(\frac{1}{2}\Delta K\right)^2 & 0 \end{pmatrix}, \quad (1)$$

where the complex number k is defined as $k = k_x + ik_y$, and $\Delta K = \Delta K_x + i\Delta K_y$. Here (k_x, k_y) is the two-dimensional wave vector $\vec{k}$ relative to the midpoint of the two Dirac points. A low-energy expansion of Hamiltonian (1) around $\pm\Delta K/2$, by defining $k = q \pm \Delta K/2$, yields two Dirac Hamiltonians $\pm(2\nu_F^2\Delta K/15\tilde{t}_\perp)\vec{\sigma}\cdot\vec{q}$, which have identical chirality as that of graphene monolayer [32]. It indicates that the low-energy tunneling behavior in twisted graphene bilayer should be similar to that in graphene monolayer. Theoretically, the continuum limit of the Hamiltonian (1) is valid for $a \ll L$ (here L is period of the moire patterns in twisted graphene bilayer), i.e., for small twist angles. In experiments, the VHSs were observed in a twisted graphene bilayer with $\theta \leq 10°$ [15,23–28]. It is, therefore, reasonable to assume that the Hamiltonian (1) is a good approximation for $\theta \leq 10°$ ($L \sim 1.4$ nm for $\theta = 10°$). The energy spectrum derived from Hamiltonian (1) is

$$E(k_x, k_y) = \pm\frac{2\nu_F^2}{15\tilde{t}_\perp}\sqrt{\left(k_x^2 - k_y^2 - \frac{1}{4}\Delta K_x^2 + \frac{1}{4}\Delta K_y^2\right)^2 + \left(2k_xk_y - \frac{1}{2}\Delta K_x\Delta K_y\right)^2}. \quad (2)$$

Obviously, the energy spectrum is symmetric between the positively and negatively charged chiral fermions; therefore we only consider the nearest neighbor hopping in Hamiltonian (1). This symmetry, which is analogous to the inherent symmetric structure between electrons and positrons of the Universe, is crucial to the chiral tunneling in all the graphene systems (including graphene monolayer, Bernal graphene bilayer, and twisted graphene bilayers) [9]. A large next-nearest-neighbor hopping breaking the symmetry of the positively and negatively charged chiral fermions is expected to destroy the chiral tunneling.

Unlike the case of single layer and Bernal bilayer graphene, the group velocity of wave packets in twisted bilayer graphene is not parallel to its wave vector any more. It could be determined by $\vec{\nu}_{k_0} = (1/\hbar)(\nabla_k E)_{k_0}$. In our calculation, we also use the rectangular shape assumption of the barrier and, consequently, intervalley scattering between different valleys in graphene can be neglected. Therefore, we only consider scattering electrons from the K and K_θ cones. The velocity field of quasiparticles with various energies is shown in Fig. S1 (see Supplemental Material [34]). Inserting a trial wave function $\Psi(x, y) = \binom{\varphi_A(x)}{\varphi_B(x)}e^{ik_y y}$ into equation $H\Psi = E\Psi$ with the Hamiltonian (1), we obtain

$$\left(\frac{2\nu_F^2}{15t_\perp}\right)^2\left[\left(k_x^2 - k_y^2 - \frac{1}{4}\Delta K_x + \frac{1}{4}\Delta K_y\right)^2 + \left(2k_xk_y - \frac{1}{2}\Delta K_x\Delta K_y\right)^2\right] = E^2. \quad (3)$$

There are four possible solutions for a given energy. Two of them are propagating waves $\exp(\pm ik_{x1}x)$ and the other two are exponentially growing and decaying modes $\exp(\pm k_{x2}x)$. Here, k_{x1} and ik_{x2} are wave vectors. The wave function in the three different regions of the tunneling problem can be written in terms of incident and reflected waves. The reflection coefficient and the transmission coefficient are determined from the continuity of the

wave functions and their derivatives (see Supplemental Material [34] for details of the analysis and calculation).

Figure 2 shows examples of the transmission probability as a function of the incident angle $T(\varphi)$ for a twisted graphene bilayer. Here we only show the transmission probability of quasiparticles in the K cone. The transmission probability of quasiparticles in the K_θ cone is mirror symmetric about $\varphi = 0°$ when the potential barrier is parallel to the line connecting K and K_θ, as shown in Fig. S1 [34]. If we change the orientation of the potential barrier, the transmission probability for the two cones becomes asymmetry about $\varphi = 0°$. However, the main result, as discussed subsequently, is valid and robust irrespective of the orientation of the barrier.

To elucidate differences and similarities of the $T(\varphi)$ between the twisted graphene bilayer and graphene monolayer, we also calculated the same tunneling problem of the system described by the Hamiltonian $(2v_F^2\Delta K/15\tilde{t}_\perp)\vec{\sigma}\cdot\vec{q}$ for comparison. For low incident energy and a small value of ΔU, the angular dependence of the transmission probability for the twisted graphene bilayer resembles that of a graphene monolayer and the chiral fermions are perfectly or almost perfectly tunneling for normal incidence. The differences emerge for large incident energy and large value of ΔU. The $T(\varphi)$ is asymmetric about $\phi = 0$ in a twisted graphene bilayer and the asymmetry increases with increasing the incident energy and the height of the barrier (see Fig. S2 of the Supplemental Material [34]). The most striking result of the tunneling problem is that the transmission probability at $\varphi = 0$ depends sensitively on the incident energy and the height of the barrier, which is quite different from that of the graphene monolayer and the Bernal graphene bilayer.

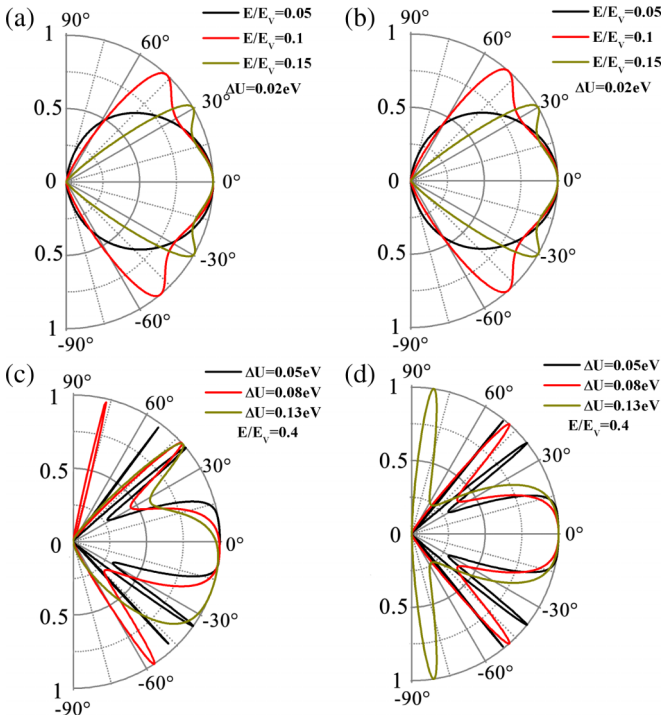

FIG. 2 (color online). Quantum tunneling in a twisted graphene bilayer for low incident energy. Transmission probability T through a 100-nm wide barrier as a function of the incident angle φ for (a),(c) a twisted graphene bilayer and (b),(d) the system described by the Hamiltonian $(2v_F^2\Delta K/15\tilde{t}_\perp)\vec{\sigma}\cdot\vec{q}$. The remaining parameters are the twist angle of the graphene bilayer $\theta = 3.89°$, $t_\perp = 0.12$ eV, and $E_V = 0.15$ eV. We only plotted the transmission of the states in a particular cone; the transmission of the corresponding states in the other cone is related by mirror symmetry. The angular behavior of $T(\varphi)$ in (b),(d) is similar to that of a graphene monolayer, and the chiral fermions are always perfectly tunneling for normal incidence irrespective of the parameters of the barrier. The $T(\varphi)$ of the twisted graphene bilayer shows both similarities and differences with respect to that of the graphene monolayer. For twisted graphene bilayers, the $T(\varphi)$ is asymmetric about $\varphi = 0$ and the asymmetry increases with increasing height of the barrier.

To further understand the chiral tunneling in a twisted graphene bilayer, we calculated the transmission probability for normally incident electrons as a function of the incident energy, as shown in Fig. 3(a). It is interesting to note that the incident energy can tune the transmission probability in a twisted graphene bilayer. This unique behavior is essentially due to the different chirality or pseudospins of the quasiparticles involved (see Fig. S3 in the Supplemental Material [34]). For a graphene monolayer and a Bernal graphene bilayer, the propagating wave functions can be written as $(1/\sqrt{2})\binom{1}{se^{i\varphi}}e^{i\vec{k}\cdot\vec{r}}$ and $(1/\sqrt{2})\times\binom{1}{se^{2i\varphi}}e^{i\vec{k}\cdot\vec{r}}$, respectively (here $s = \mathrm{sgn}E$). The $e^{i\varphi}$ and $e^{2i\varphi}$ can be viewed as the phase difference between the two components of the "spinor wave functions," which is independent of the incident energy. The perfect matching between an incident electron wave function and the corresponding wave function for a propagating hole inside a barrier at the barrier interface yields $T = 1$ in a graphene monolayer. For a Bernal graphene bilayer, the propagating electron wave function transforms into an evanescent hole wave function inside the barrier, resulting in the perfect reflection for a wide barrier [9]. However, for the case of a twisted graphene bilayer, the propagating wave function has the form $(1/\sqrt{2})\binom{1}{sq_1^+}e^{i\vec{k}\cdot\vec{r}}$ and the term q_1^+ is energy dependent (see Supplemental Material [34]). The q_1^+ of the wave function approaches $e^{i\varphi}$ around the Dirac points and is a good approximation of $e^{2i\varphi}$ for the high-energy spectrum. Therefore, the transmission probability in a twisted graphene bilayer is a function of the incident energy and can be changed from perfect tunneling to complete reflection, as shown in Fig. 3(a). The normal tunneling becomes completely forbidden for incident energy higher than $2E_V$ because the quasiparticles in the twisted graphene bilayer become the pseudospin-1 fermions exactly for $E \geq 2E_V$ (see Supplemental Material [34] for details of the discussion).

We also studied the transmission probability in a twisted graphene bilayer as a function of the potential barrier $U(x)$, as shown in Fig. 3(b). Here the height of potential barrier

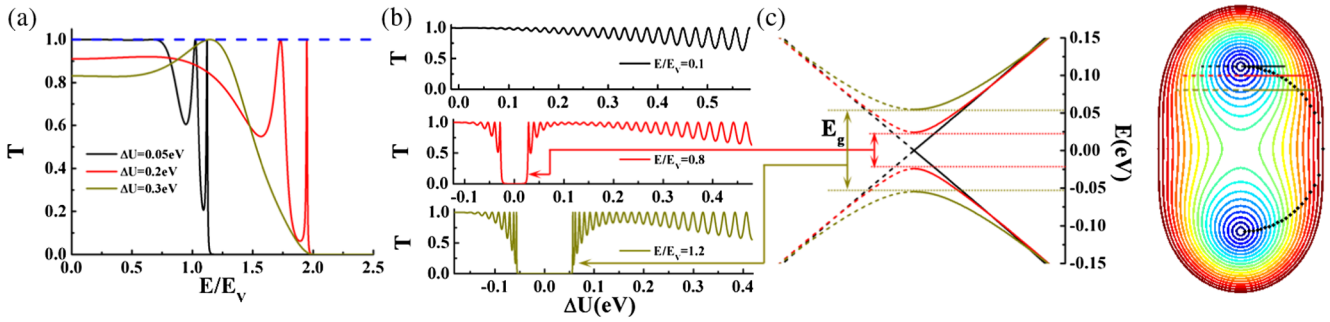

FIG. 3 (color online). Quantum tunneling in a twisted graphene bilayer for normally incident electrons. (a) Transmission probability for normally incident electrons as a function of the incident energy. The curves with different colors correspond to different values of the ΔU. (b) Transmission probability for normally incident electrons with different incident energy as a function of the value of ΔU. Here the height of potential barrier $U(x)$ increases from zero; i.e., the value of ΔU increases from $-E$. In the middle and lower panels, the transmission is completely suppressed when $|\Delta U| < E_g/2$ [E_g is defined in panel (c)]. For a certain value of ΔU (here $\Delta U > E_g/2$), the amplitude of the oscillations increases with the incident energy. For a fixed incident energy, both the periodicity and the amplitude of the oscillations increase with the positive value of ΔU (here $\Delta U > E_g/2$). (c) The right panel is a density plot of the energy dispersion of the twisted graphene bilayer around K and K_θ. The dark dots are the positions of normal incident electrons in the superlattice Brillouin zone. The energy spectra in the left panel are a section view of band structures through serifs that cross normal incident modes. The dashed curves represent the electrons that are moving away from the barrier in the perpendicular direction.

$U(x)$ increases from zero, i.e., the value of ΔU increases from $-E$. The chiral electrons in the twisted graphene bilayer combine the two distinct behaviors of quasiparticles in the graphene monolayer and the Bernal graphene bilayer. Usually, both the propagation hole state and the exponential decaying mode coexist inside the potential barrier, and the weights of the two components can be tuned by the potential barrier. Therefore, the transmission probability can be changed from perfect tunneling to partial reflection, or vice versa, as shown in Fig. 3(b). As the amplitude of the oscillating tunneling is amplified with the increase of the value of ΔU, it is expected to see that the transmission probability can be switched between $T = 1$ and $T = 0$, which corresponds to what the chiral electron transforms into—either a propagating hole or an evanescent hole inside the barrier, respectively (see Supplemental Material [34]).

The middle and lower panels of Fig. 3(b) show a peculiar behavior of the chiral tunneling: the transmission probability is zero for a small $|\Delta U|$. This peculiar behavior can be attributed to the failure in creation of an electron-hole (''positron'') pair at the barrier interface. The translational symmetry of the potential barrier conserves the y component of wave vector (k_y) in the tunneling process. It indicates that the section cut of the energy spectrum for normal incident electrons should keep k_y a constant, as shown in Fig. 3(c). A gap E_g between electrons and holes is introduced into the energy serif of quasiparticles with large incident energies. A small potential barrier, $|\Delta U| < E_g/2$, cannot overcome the energy gap to excite holes in the classical forbidden area, so the wave vector inside the potential is imaginary, inhibiting the propagation, as shown in Fig. 3(b). This behavior is closely connected to Klein's original paradox in which a potential step of twice the rest energy of an electron (the energy ''gap'' between electrons and positrons) is required for the observation of chiral tunneling [35,36]. For the case $-E < \Delta U < -E_g/2$, the quasiparticles behave like massive Schrödinger electrons and their transmission probability oscillates because of the resonance condition [9].

The periodicity of the oscillations, as shown in Fig. 3(b), increases with increasing the value of ΔU. This effect can be explained with the help of the quantum confinement of the propagating wave functions inside the barrier. When the electron wave function perfectly matches the wave function for a propagating hole, the barrier is transparent. The energy interval between the nearest states of the propagating hole wave functions inside the barrier is proportional to the height of the barrier. As a consequence, the periodicity of the transmission probability increases with the height of barrier. To further confirm the above analysis, it is helpful to consider the same tunneling problem with different width of the barrier. The energy interval between the nearest states of the propagating hole wave functions inside the barrier is expected to increase linearly with the inverse of the width of the barrier D^{-1}. Therefore, the periodicity of the oscillations should increase linearly with D^{-1}, which is confirmed explicitly by the result shown in Fig. 4.

The perfect chiral tunneling of a graphene monolayer inhibits the fabrication of standard semiconductor devices because field-effect transistors made from graphene monolayers remain conducting even when switched off [2]. The ability to control the transmission of quasiparticles through a barrier in a twisted graphene bilayer suggests that this effect can be used as the basis for future graphene device electronics. Experimentally, a potential barrier can be easily created by the electric field effect and the parameter of the barrier is tunable. Therefore, the predicted effect explained in this Letter is expected to be realized in the near future.

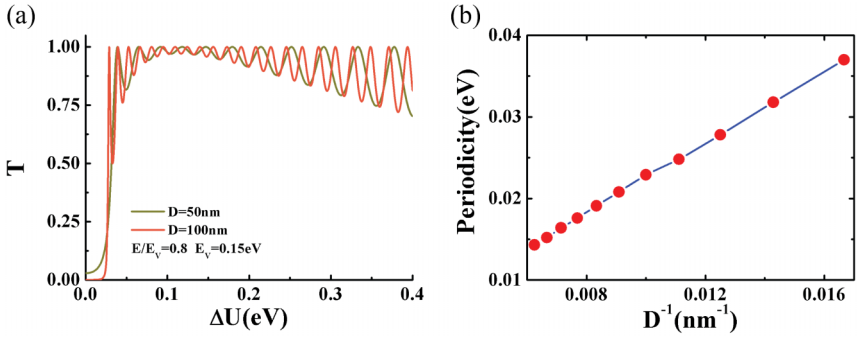

FIG. 4 (color online). Quantum tunneling in a twisted graphene bilayer with different width of the barrier. (a) Transmission probability as a function of the values of the ΔU. The curves with different colors correspond to different widths of the barriers. (b) The average periodicity of the oscillations for $0.3\ \mathrm{eV} < \Delta U < 0.4\ \mathrm{eV}$ as a function of D^{-1}. Here D is the width of the barrier. The periodicity almost increases linearly with D^{-1}.

We are grateful to National Key Basic Research Program of China (Grant No. 2013CBA01603, No. 2014CB920903), National Science Foundation (Grant No. 11004010), and the Fundamental Research Funds for the Central Universities.

*helin@bnu.edu.cn

[1] K. S. Novoselov, A. K. Geim, S. V. Morozov, D. Jiang, Y. Zhang, S. V. Dubonos, I. V. Grigorieva, and A. A. Firsov, Science **306**, 666 (2004).
[2] A. K. Geim and K. S. Novoselov, Nat. Mater. **6**, 183 (2007).
[3] A. H. Castro Neto, N. M. R. Peres, K. S. Novoselov, and A. K. Geim, Rev. Mod. Phys. **81**, 109 (2009).
[4] M. A. H. Vozmediano, M. I. Katsnelson, and F. Guinea, Phys. Rep. **496**, 109 (2010).
[5] S. Das Sarma, S. Adam, E. Hwang, and E. Rossi, Rev. Mod. Phys. **83**, 407 (2011).
[6] K. S. Novoselov, A. K. Geim, S. V. Morozov, D. Jiang, M. I. Katsnelson, I. V. Grigorieva, S. V. Dubonos, and A. A. Firsov, Nature (London) **438**, 197 (2005).
[7] Y. Zhang, Y. W. Tan, H. L. Stormer, and P. Kim, Nature (London) **438**, 201 (2005).
[8] M. Goerbig, Rev. Mod. Phys. **83**, 1193 (2011).
[9] M. I. Katsnelson, K. S. Novoselov, and A. K. Geim, Nat. Phys. **2**, 620 (2006).
[10] C. Bai and X. D. Zhang, Phys. Rev. B **76**, 075430 (2007).
[11] A. F. Young and P. Kim, Nat. Phys. **5**, 222 (2009).
[12] M. I. Katsnelson and K. S. Novoselov, Solid State Commun. **143**, 3 (2007).
[13] M. A. H. Vozmediano, M. I. Katsnelson, and F. Guinea, Phys. Rep. **496**, 109 (2010).
[14] M. Yankowitz, J. Xue, D. Cormode, J. D. Sanchez-Yamagishi, K. Watanabe, T. Taniguchi, P. Jarillo-Herrero, P. Jacquod, and B. J. LeRoy, Nat. Phys. **8**, 382 (2012).
[15] T. Ohta, J. T. Robinson, P. J. Feibelman, A. Bostwick, E. Rotenberg, and T. E. Beechem, Phys. Rev. Lett. **109**, 186807 (2012).
[16] H. Yan, Z.-D. Chu, W. Yan, M. Liu, L. Meng, M. Yang, Y. Fan, J. Wang, R.-F. Dou, Y. Zhang, Z. Liu, J.-C. Nie, and L. He, Phys. Rev. B **87**, 075405 (2013).
[17] C.-H. Park, L. Yang, Y.-W. Son, M. L. Cohen, and S. G. Louie, Nat. Phys. **4**, 213 (2008).
[18] C.-H. Park, L. Yang, Y.-W. Son, M. L. Cohen, and S. G. Louie, Phys. Rev. Lett. **101**, 126804 (2008).
[19] M. Killi, S. Wu, and A. Paramekanti, Phys. Rev. Lett. **107**, 086801 (2011).
[20] Z.-D. Chu, W. Y. He, and L. He, Phys. Rev. B **87**, 155419 (2013).
[21] J. M. B. Lopes dos Santos, N. M. R. Peres, and A. H. Castro Neto, Phys. Rev. Lett. **99**, 256802 (2007).
[22] J. M. B. Lopes dos Santos, N. M. R. Peres, and A. H. Castro Neto, Phys. Rev. B **86**, 155449 (2012).
[23] G. Li, A. Luican, J. M. B. Lopes dos Santos, A. H. Castro Neto, A. Reina, J. Kong, and E. Y. Andrei, Nat. Phys. **6**, 109 (2009).
[24] A. Luican, G. Li, A. Reina, J. Kong, R. Nair, K. Novoselov, A. Geim, and E. Andrei, Phys. Rev. Lett. **106**, 126802 (2011).
[25] W. Yan, M. Liu, R.-F. Dou, L. Meng, L. Feng, Z.-D. Chu, Y. F. Zhang, Z. F. Liu, J.-C. Nie, and L. He, Phys. Rev. Lett. **109**, 126801 (2012).
[26] I. Brihuega, P. Mallet, H. Gonzalez-Herrero, G. T. Laissardiere, M. M. Ugeda, L. Magaud, J. M. Gomez-Rodriguez, F. Yndurain, and J.-Y. Veuillen, Phys. Rev. Lett. **109**, 196802 (2012).
[27] L. Meng, Z.-D. Chu, Y. Zhang, J.-Y. Yang, R.-F. Dou, J.-C. Nie, and L. He, Phys. Rev. B **85**, 235453 (2012).
[28] K. Kim, S. Coh, L. Tan, W. Regan, J. Yuk, E. Chatterjee, M. Crommie, M. Cohen, S. Louie, and A. Zettl, Phys. Rev. Lett. **108**, 246103 (2012).
[29] O. Vafek and K. Yang, Phys. Rev. B **81**, 041401(R) (2010).
[30] F. Zhang and A. H. MacDonald, Phys. Rev. Lett. **108**, 186804 (2012).
[31] Y. Lemonik, I. L. Aleiner, C. Toke, and V. I. Fal'ko, Phys. Rev. B **82**, 201408(R) (2010).
[32] R. de Gail, M. O. Goerbig, F. Guinea, G. Montambaux, and A. H. Castro Neto, Phys. Rev. B **84**, 045436 (2011).
[33] M. Y. Choi, Y. H. Hyun, and Y. Kim, Phys. Rev. B **84**, 195437 (2011).
[34] See Supplemental Material at http://link.aps.org/supplemental/10.1103/PhysRevLett.111.066803 for details of the discussion and analysis.
[35] R. Nandkishore, and L. Levitov, Proc. Natl. Acad. Sci. U.S.A. **108**, 14 021 (2011).
[36] T. Tudorovskiy, K. J. A. Reijnders, and M. I. Katsnelson, Phys. Scr. **T146**, 014010 (2012).